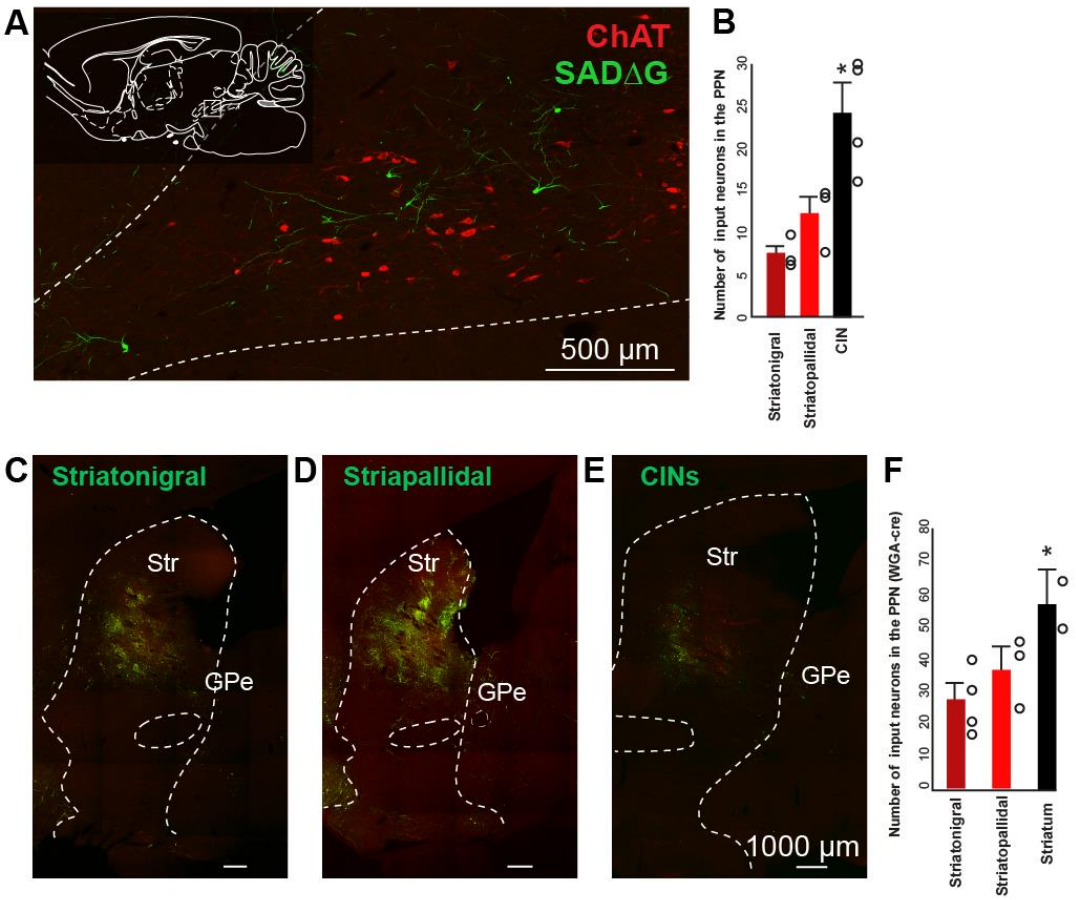

Figure S1: Low magnification images of tracing experiments. Related to Figure 1.

(A) Low magnification image of input neurons in the PPN. Square in the inset outline shows the location within the PPN.

(B) Quantification of total input neurons in the PPN and LDT (each circle represents one rat, obtained from 3 rats in striatonigral and striatopallidal labeling, and 4 rats in CINs). * $P < 0.05$ (statistical details in the text).

(C-E) Low magnification images showing of the extent of viral diffusion labeling of starter neurons.

(F) Normalized quantification of input neurons in the PPN and LDT using WGA-Cre instead of Cav2 (n = 4 rats in striatonigral, n = 3 striatopallidal, n = 2 all striatal cells). * $P < 0.05$ (statistical details in the text).

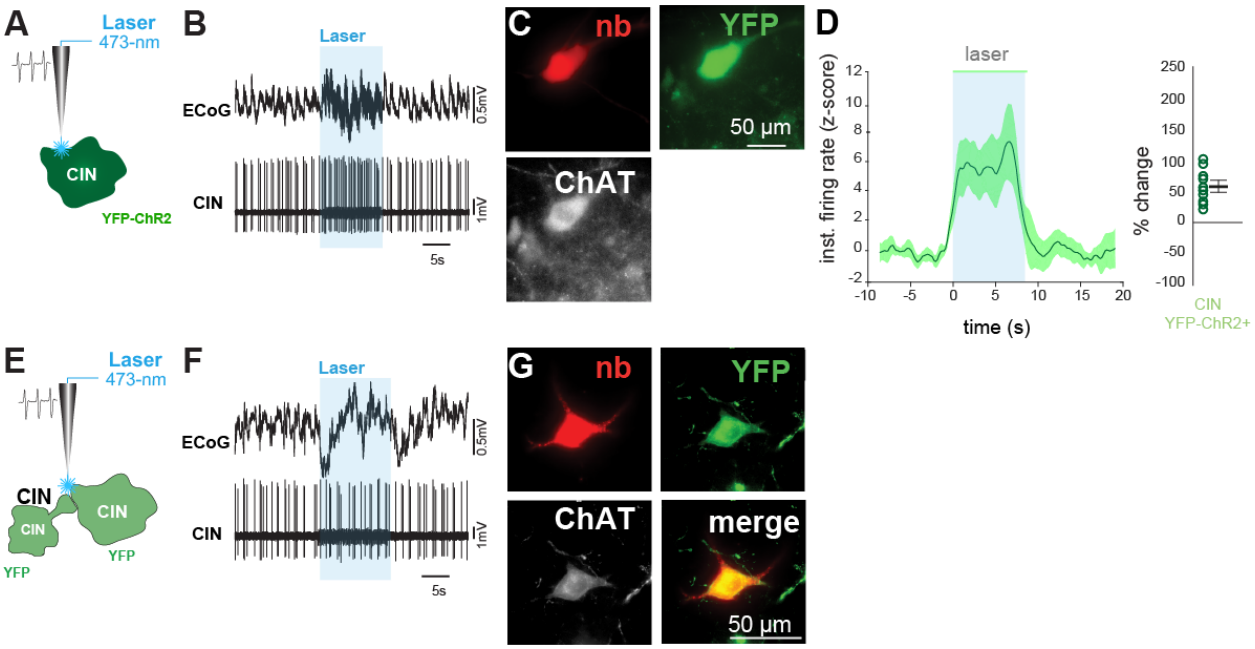

Figure S2. Controls for optogenetic experiments. Related to Figures 2 and 3.

(A) AAV-DIO-EF1a-eYFP-ChR2 or (E) AAV-DIO-eYFP injected in the striatum of ChAT::cre+ rats. (B) YFP-ChR2-positive CINs (n = 11) or (F) YFP-positive CINs (n = 11) were recorded with a glass micropipette and blue light was delivered to the recorded neurons. (C) YFP-ChR2-positive or (G) YFP-positive somata were found around the recording site and were revealed by ChAT immunostaining. (D) The normalized instantaneous firing rate of all CINs expressing ChR2-YFP show fast activation dynamics during stimulation (cluster-based permutation test, $P < 0.001$). A significant increase of the firing rate was observed for animals injected with AAV-DIO-ChR2-YFP (firing rate: before laser stimulation 3.9 ± 1.28 Hz; during laser stimulation 6.14 ± 1.43 Hz; after laser stimulation 4.046 ± 1.32 Hz, paired t-test before vs. after: $t(10) = -3.588$, $P = 0.005$) but not for animals injected with AAV-DIO-YFP (firing rate: before laser stimulation 4.92 ± 2.19 Hz, during laser stimulation 4.95 ± 2.20 Hz, after laser stimulation 4.94 ± 2.15 Hz, n = 11 neurons in 4 animals; paired t-test before vs. after: $t(10) = -0.587$, $P = 0.570$; data not shown).

Individual data points and mean ± SEM are shown. * $P < 0.05$.

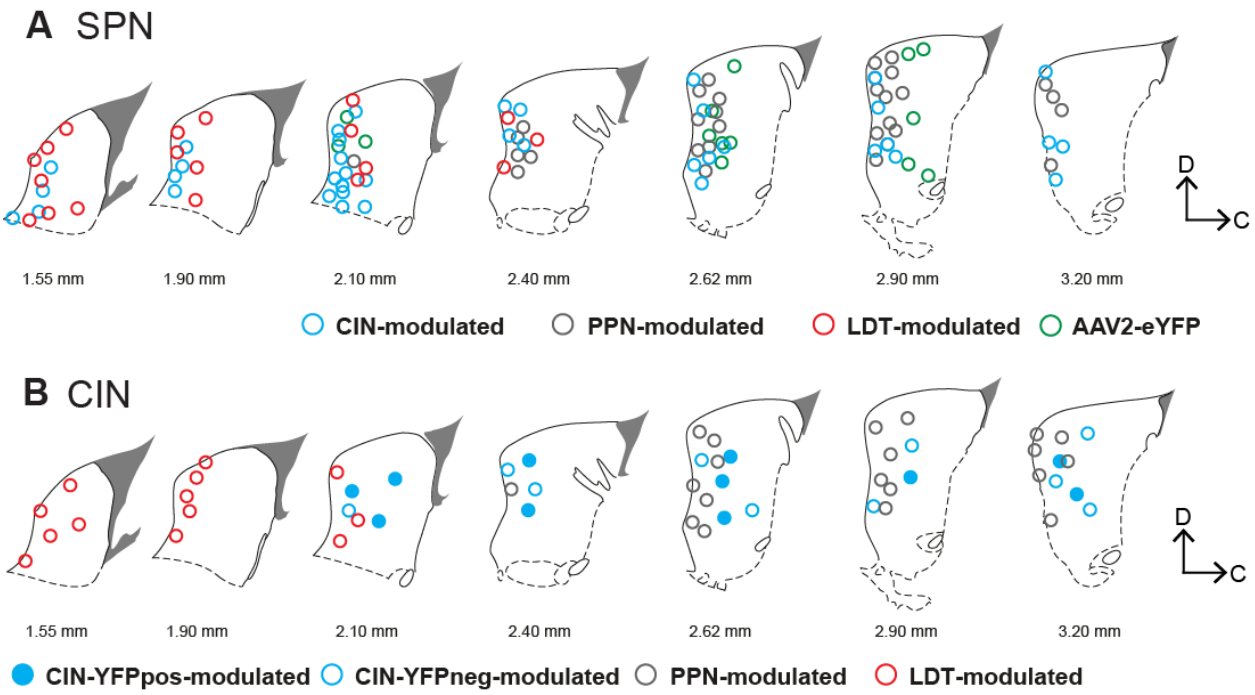

Figure S3. Localization of recorded neurons in the striatum. Related to Figures 2 and 3.

Localization of recorded and subsequently labeled neurons in the striatum confirmed as SPNs (A) or CINs (B), following CINs stimulation (blue circles), PPN stimulation (gray circles), LDT stimulation (red circles) or control animals (green circles). Neurons are represented on medial to lateral sagittal planes of the striatum; approximate medio-lateral coordinates from Bregma are provided.

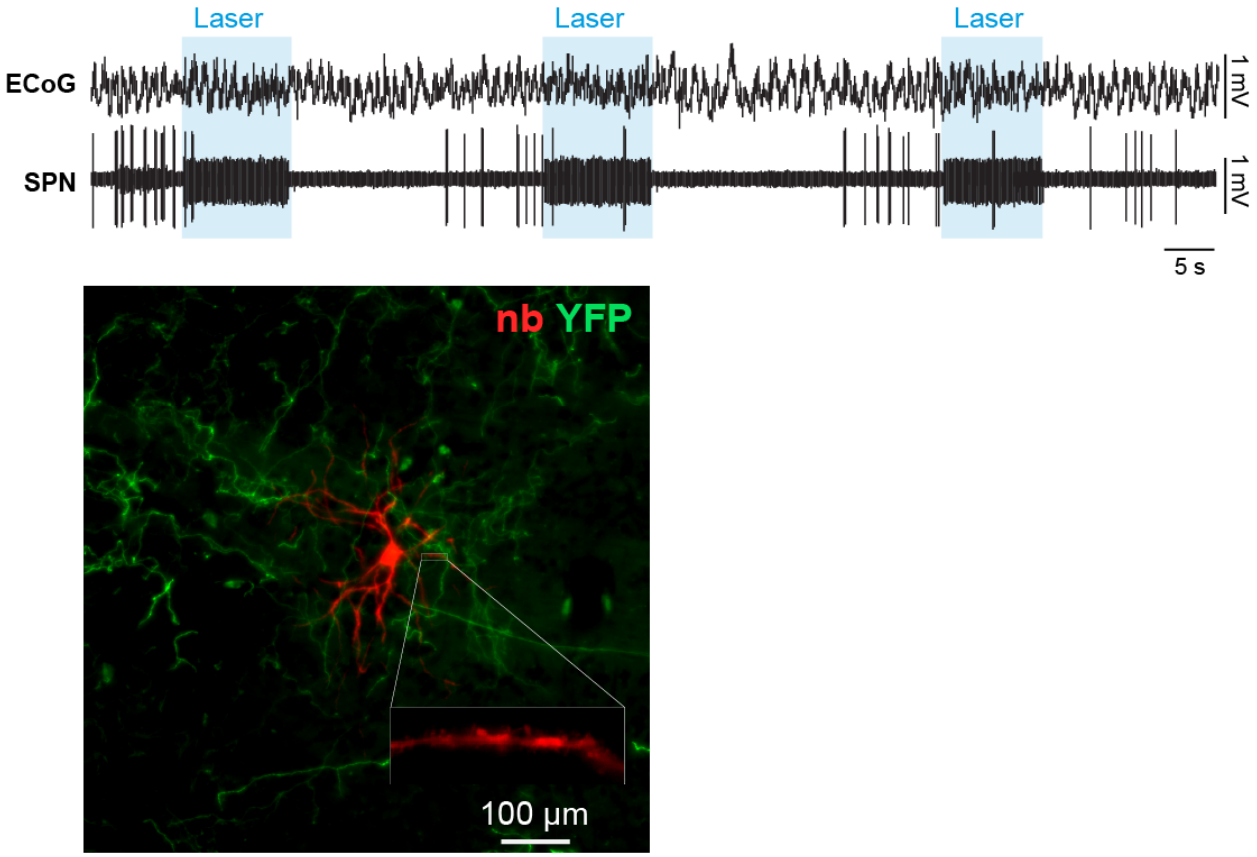

Figure S4: Extended recording of a SPN. Related to Figure 2.

Individual identified SPN neuron activity during 3 subsequent stimulation trials of PPN cholinergic axons in the striatum. This neuron was surrounded by YFP-positive axons.

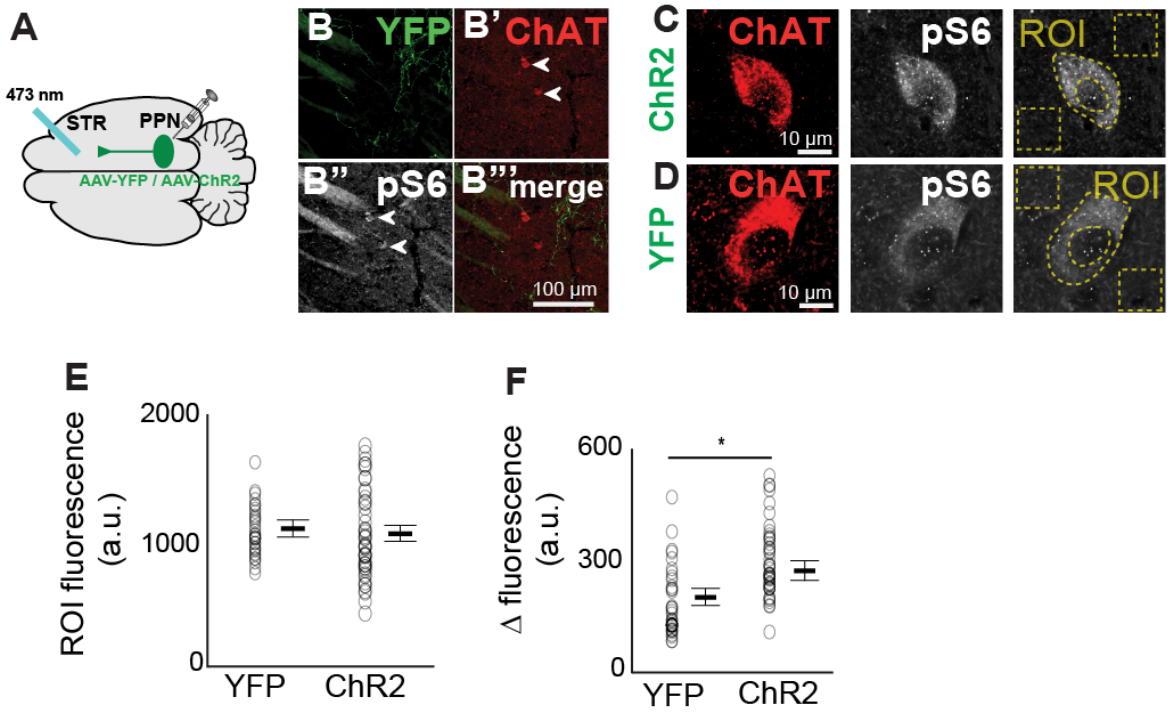

Figure S5. Increase in the phosphorylation of serine 240-244 in CINs following activation of midbrain cholinergic axons. Related to Figure 3.

(A) Schematic of the experiment showing optogenetic stimulation of striatal neurons in ChAT::cre rats injected with AAV-DIO-ChR2-YFP (5 rats) or AAV-DIO-YFP (controls; 5 rats) in the midbrain.

(B) Low magnification confocal images showing presence of transduced cholinergic axons from the midbrain in the vicinity of CINs (B') that are co-expressing $pSer^{240-244}$ (pS6) (B'').

(C, D) High magnification confocal images showing $pSer^{240-244}$ intensity in CINs following blue laser stimulation of ChR2-YFP- (C) or YFP-transduced (D, controls) cholinergic midbrain axons in the striatum.

No differences were observed in the expression of $pSer^{240-244}$ signal in region of interest (ROI) selected as background (E, paired t-test, $P > 0.05$), whereas a significant difference was found in the contrast between ROI and soma (F_{SOMA}-F_{ROI}) fluorescence (F; 165 neurons, one way ANOVA $F(1,163) = 18.522$, $P = 0.000029$) following laser stimulation of YFP or ChR2-YFP- expressing cholinergic midbrain axons in the striatum.

Individual data points and mean ± SEM are shown. * $P < 0.05$.

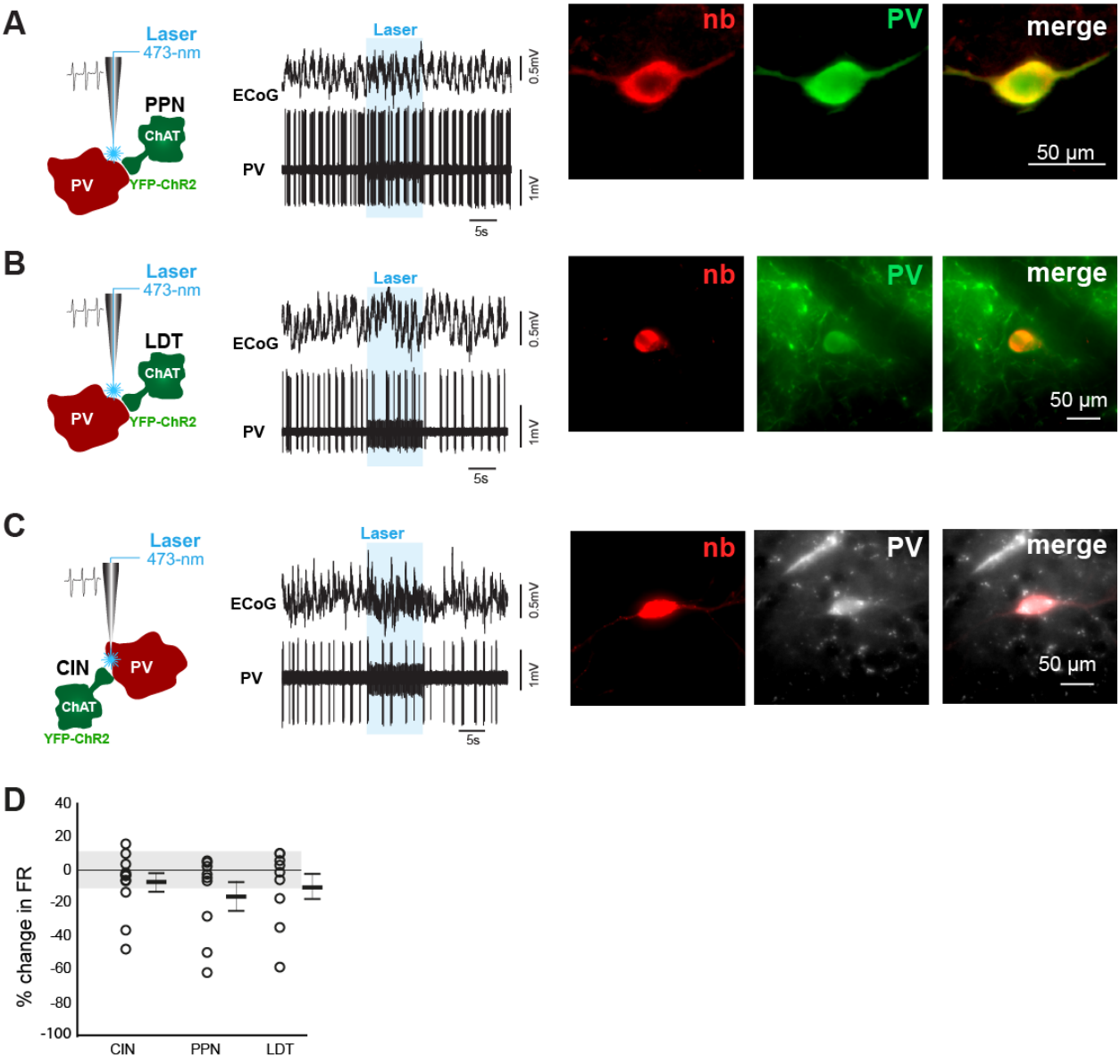

Figure S6. Optogenetic activation of cholinergic inputs does not modulate parvalbumin-expressing (PV) interneuron firing rates. Related to Figures 2 and 3.

(A) AAV-DIO-EF1a-eYFP-ChR2 injected in the PPN of ChAT::cre+ rats. PV interneurons in the striatum were recorded with a glass micropipette and the cholinergic axons were stimulated optogenetically (n = 8 neurons). Individual recordings were obtained and the cells were subsequently revealed with neurobiotin and neurochemically characterized.

(B) Same experimental design to assess modulation of striatal PV interneurons by LDT cholinergic axons (n = 9 neurons).

(C) Same experimental design to assess modulation of striatal PV interneurons by cholinergic axons arising from local CINs in the dorsal striatum (n = 11 neurons).

(D) No differences in the firing activity of PV-positive neurons recorded across groups were observed (PPN: 8.55 ± 2.66 Hz; LDT: 7.16 ± 1.42 Hz; CIN: 8.43 ± 2.47 Hz; one-way ANOVA, $F_{(2,25)} = 0.11$, $P = 0.8968$; data not shown). Following photostimulation of cholinergic axons no differences were found in the changes in the firing rates (D, CIN: 1.084 ± 18.58 %, PPN: -1.38 ± 15.91 %, LDT: -3.14 ± 11.56 %; one-way ANOVA: $F_{(2,25)} = 0.70$, $P = 0.5$).

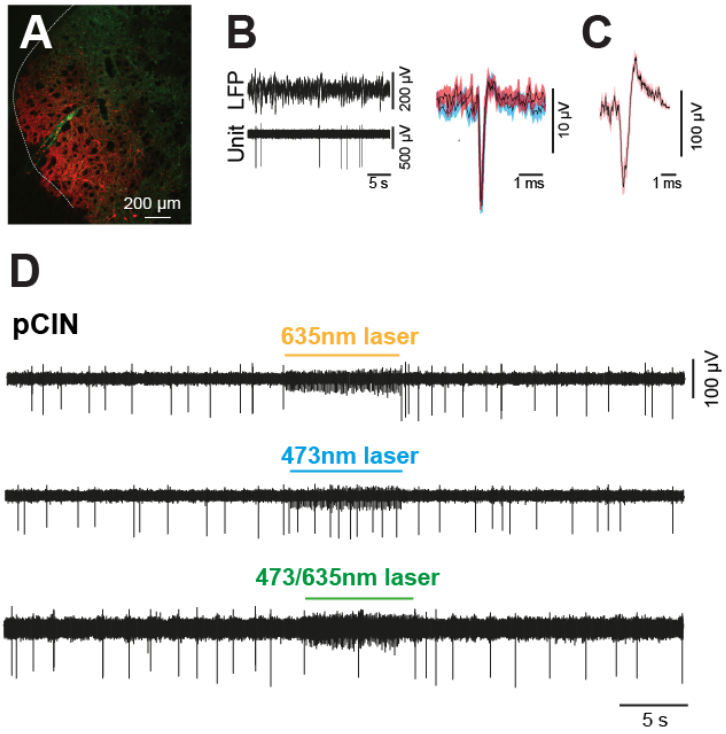

Figure S7: *In vivo* extracellular recordings in the striatum. Related to Figure 4.

(A) Low-magnification fluorescent image of an overlapping area of striatum containing cholinergic PPN/LDT axons (YFP) and CINs (mCherry).

(B, C) Representative examples of a putative SPN (B, pSPN) or a putative CIN (C, pCIN) recorded using 16-channels silicon probes. pSPN and pCIN firing activity in multi-contact recordings was similar to that observed in juxtacellularly recorded neurons that were subsequently identified as SPNs or CINs (the trace in B belongs to a pSPN). The average waveform of a pSPN in B during baseline conditions (red) and light stimulation (blue) suggests that there is no effect of the laser stimulation on spike properties in multi-contact extracellular recordings.

(D) Response of a representative pCIN expressing NphR3.0-mCherry following yellow (635 nm), blue (475 nm) or combined yellow/blue laser stimulation. pCINs were inhibited by yellow light (top trace) and excited by blue light (middle trace).

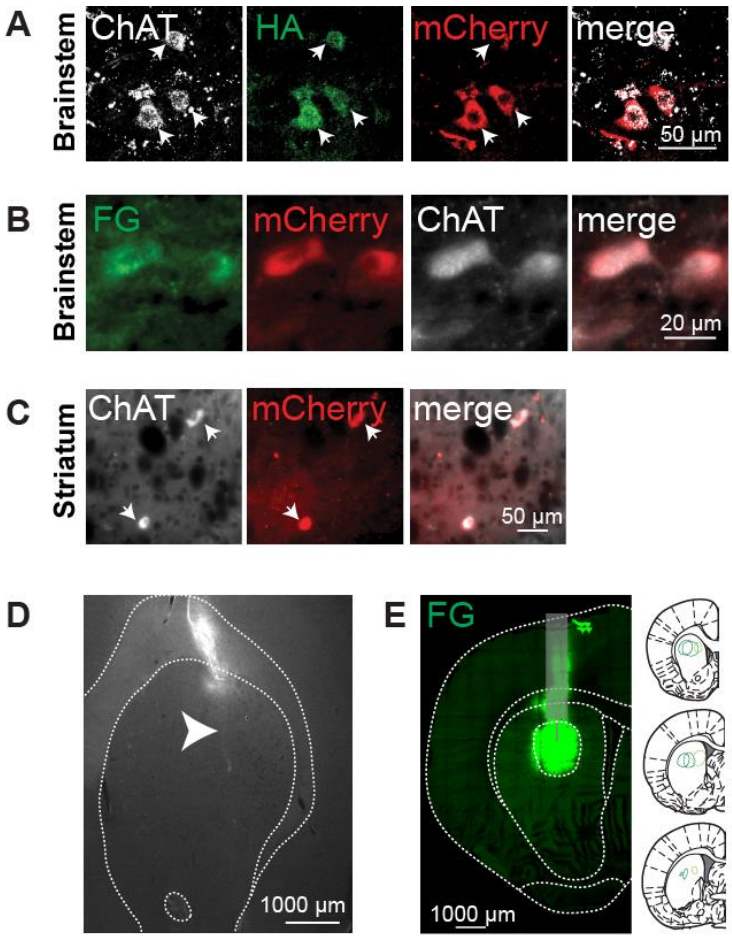

Figure S8. Histology from behavioral experiments. Related to Figures 5 and 6.

(A) Following injection of AAV-DIO-Hm4Di-HA-mCherry in the cholinergic midbrain, expression of mCherry and HA were observed only in neurons positively labeled for ChAT.

(B) Cholinergic neurons in the midbrain expressing mCherry were retrogradely-labeled following injection of Fluorogold (FG) through the cannula in the striatum used for CNO delivery.

(C) Following injection of AAV-DIO-Hm4Di-HA-mCherry in the striatum, expression of mCherry was observed only in neurons positively labeled for ChAT. No retrograde mCherry labeling was observed in the midbrain.

(D) Location of the cannula in the striatum (DLS in this example) determined by FG.

(E) Diffusion of FG in the striatum. The volume of FG was the same as the volume of CNO to determine the extent of diffusion within the striatum (see text for details).

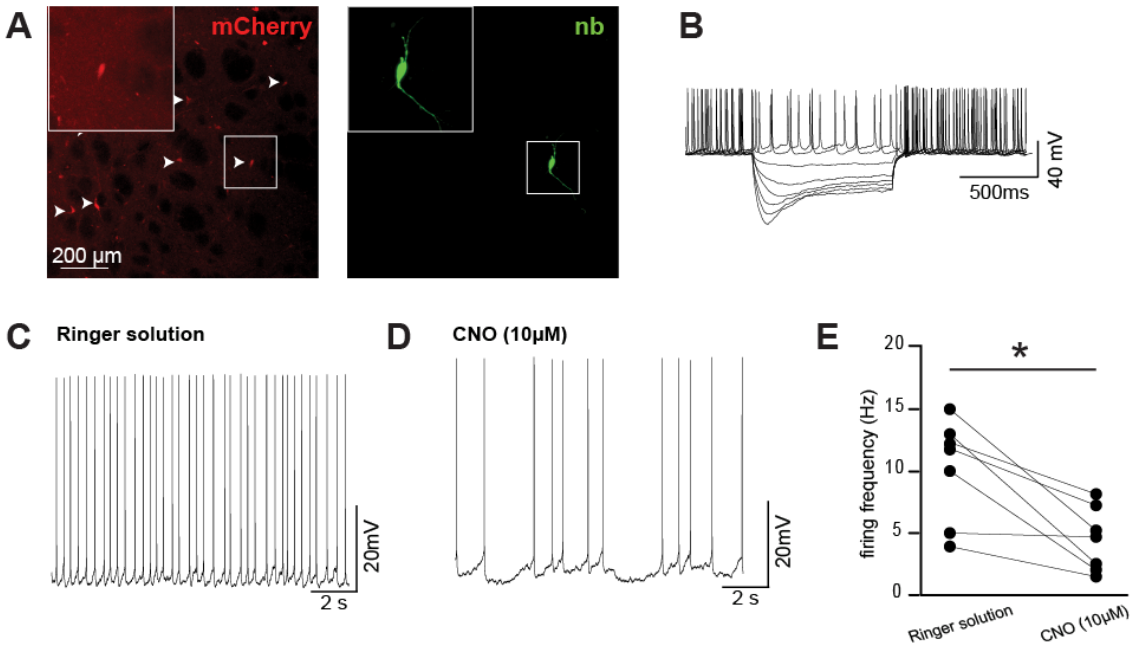

Figure S9: Effect of CNO administration on *in vitro* firing activity of CINs. Related to Figures 5 and 6.

(A-E) Whole cell current clamp recordings of identified CINs expressing tdTomato (n = 7 neurons) before (C) and after (D) bath application of CNO (clozapine-N-oxide, 10µM). A significant decrease in the neuron activity was observed (paired t-test: t(6) = 3.677, *P* = 0.0104).

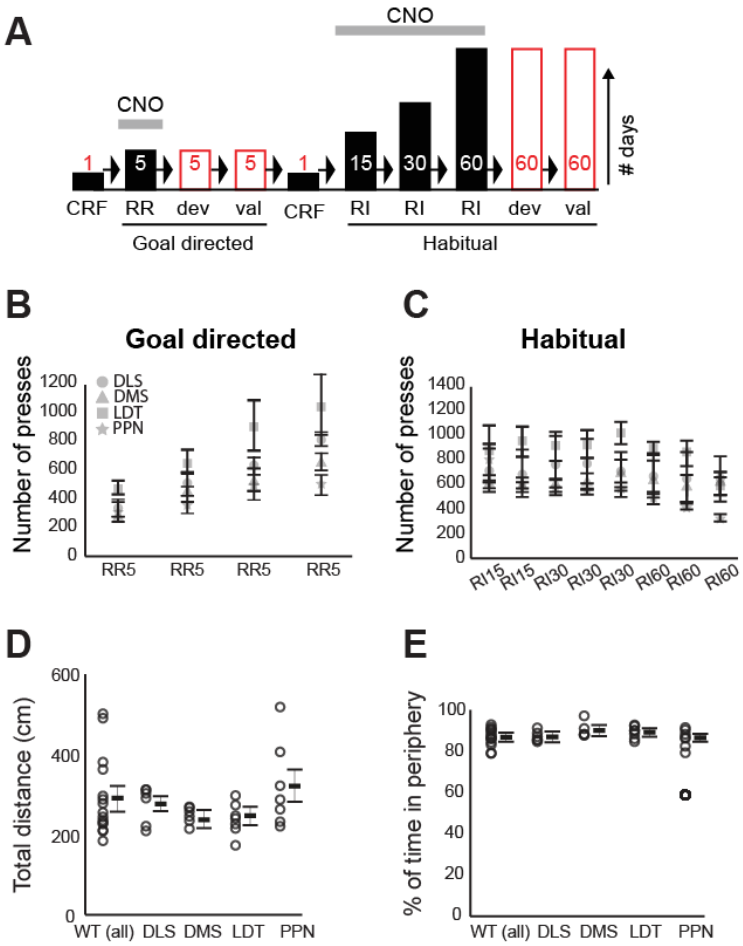

Figure S10. Design of behavioral experiments. Related to Figure 5 and 6.

(A) Schematic of the experimental design illustrating the training and the timing of intracranial CNO administration. The height of the bars represents the number of experimental days.

(B-C) Acquisition of lever press in control (WT) rats under RR (B) and RI (C) contexts revealed no significant differences in the number of lever presses between groups (see text for statistical values).

(D-E) Effect of virus injections and CNO on locomotion (D) or anxiety related behavior (E) revealed no significant effects across groups (see text for statistical values).

Individual data points and mean ± SEM are shown.

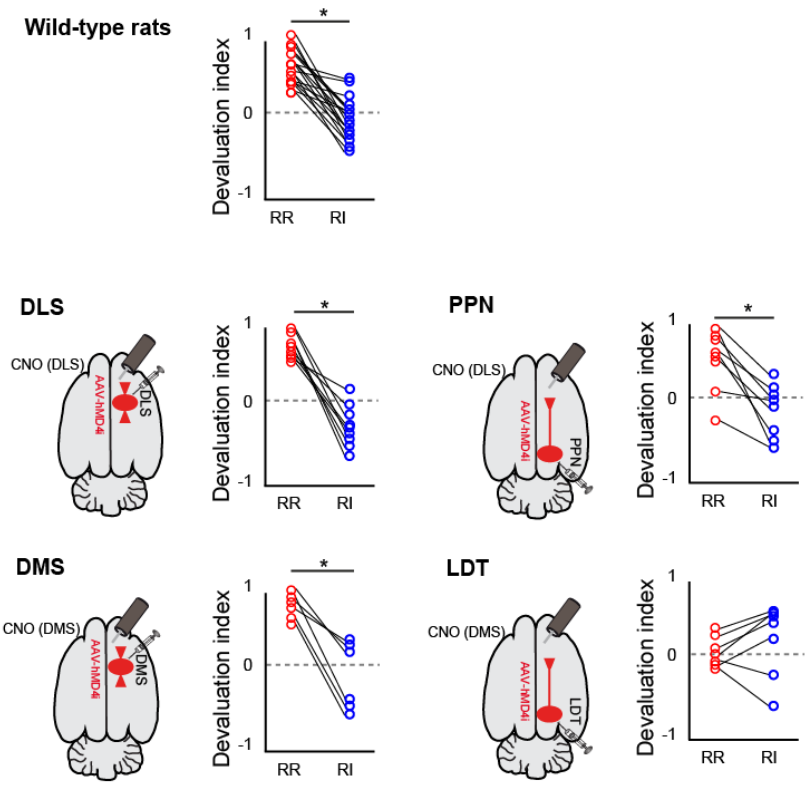

Figure S11. Devaluation index of the number of presses. Related to Figures 5 and 6.

The difference in the proportion of responses between valued and devalued sessions was calculated from the normalized number of presses and obtained as an index. This difference (devaluation index) was significantly different in all groups except the LDT group (paired t-test: DLS $t(8) = 7.704$, $P = 0.000057$; PPN $t(7) = 2.739$, $P = 0.029$; DMS $t(5) = 4.299$, $P = 0.008$).